JGR Space Physics

RESEARCH ARTICLE
10.1029/2025JA033860

# Dawn-Dusk Morphology of Auroral Arcs in Substorm Growth Phase

**Zepeng Liu[1], San Lu[1,2,3], Y. Nishimura[4], Quanming Lu[1,2,3], Boyi Wang[5], Yuzhang Ma[6], Zhibo Zhang[1], Rongsheng Wang[1,2,3], Rajkumar Hajra[1], S. Apatenkov[7], E. Grigorenko[8], A. V. Artemyev[9], and V. Angelopoulos[9]**

[1]CAS Key Laboratory of Geospace Environment, School of Earth and Space Sciences, CAS Center for Excellence in Comparative Planetology, University of Science and Technology of China, Hefei, China, [2]Deep Space Exploration Laboratory, Hefei, China, [3]Collaborative Innovation Center of Astronautical Science and Technology, Harbin, China, [4]Department of Electrical and Computer Engineering and Center for Space Physics, Boston University, Boston, MA, USA, [5]Institute of Space Science and Applied Technology, Harbin Institute of Technology (Shenzhen), Shenzhen, China, [6]Shandong Provincial Key Laboratory of Optical Astronomy and Solar-Terrestrial Environment, Institute of Space Sciences, Shandong University, Weihai, China, [7]Earth's Physics Department, Saint Petersburg State University, St. Petersburg, Russia, [8]Space Research Institute of RAS, Moscow, Russia, [9]Department of Earth, Planetary, and Space Sciences, University of California, Los Angeles, CA, USA

**Key Points:**

- Morphological characteristics of substorm growth phase arcs are studied
- A latitudinal minimum of the auroral arc is developed on the duskside at the end of the growth phase
- Such dawn-dusk asymmetry is consistent with those of magnetotail current sheet thickness and substorm onset

**Supporting Information:**

Supporting Information may be found in the online version of this article.

**Correspondence to:**

S. Lu,
lusan@ustc.edu.cn

**Citation:**

Liu, Z., Lu, S., Nishimura, Y., Lu, Q., Wang, B., Ma, Y., et al. (2025). Dawn-dusk morphology of auroral arcs in substorm growth phase. *Journal of Geophysical Research: Space Physics*, *130*, e2025JA033860. https://doi.org/10.1029/2025JA033860

Received 19 FEB 2025
Accepted 19 JUL 2025

**Abstract** The substorm growth phase plays a critical role in magnetospheric energy storage through magnetotail plasma sheet thinning and magnetic flux loading, and the study of auroral morphology and structure helps us understand the process of magnetotail energy accumulation and release. This study focuses on quiescent auroral arcs, which characterizes the growth phase of substorms and precedes the subsequent expansion thereon; we utilize the observational data from Time History of Events and Macroscale Interactions (THEMIS) all-sky imagers and obtain 47 substorm growth phase arcs from 2014 to 2022. We find that the auroral arcs typically maintain structural stability, and most of them (~72.3%) move equatorward in the growth phase during which a latitudinal minimum is recorded on the duskside. Statistical examination of the 47 distinct substorm events confirms this dawn-dusk asymmetry in growth phase arc distribution. Such morphology of the growth phase arcs may originate from the magnetotail current sheet that is thinner on the duskside, we propose that this morphological characteristic likely reflects the dusk-favored magnetotail current sheet thinning process, constituting a systematic duskside preference in magnetospheric dynamics that may originate from the interplay between solar wind-magnetosphere coupling and the Hall current system in the magnetotail.

## 1. Introduction

Substorms are large-scale common disturbances in the magnetosphere, which are caused by the interaction between Earth's magnetic field and the solar wind (Akasofu, 1964). Substorms begin with a growth phase, which typically starts from the abrupt southward turning of the interplanetary magnetic field (IMF) and lasts tens of minutes until the onset of auroral expansion (Akasofu et al., 2010; Caan et al., 1977; Cowley & Lockwood, 1992; Foster et al., 1971; Gjerloev et al., 2003; Kallio et al., 2000; Kamide & Kokubun, 1996; McPherron, 1970; Motoba et al., 2015; Nishimura et al., 2010). In the substorm growth phase, solar wind entry and global convection cause excess energy storage and magnetic field stretching in the magnetotail, which makes the magnetotail current sheet thinner and the current density more intense (Caan et al., 1973, 1975; Fairfield et al., 1981). Such a current sheet corresponds to an auroral arc through mapping of the field-aligned currents (Chen et al., 2022; Nishimura et al., 2012; Pulkkinen et al., 1991).

As one of the most important characteristics of the substorm growth phase, the growth phase arcs are described as east–west elongated stable structures, which can be observed in the midnight sector. They typically extend across the all-sky imager (ASI) field of view (FOV) or at least a large part of it, with widths on the order of kilometers to hundreds of kilometers (Borovsky, 1993; Kauristie et al., 2001; Knudsen et al., 2001). In the growth phase, the magnetotail current sheet thins with the thickness decreases from several Earth radii to the sub-Earth-radius scale (Baker et al., 1996; McPherron, 1979; McPherron et al., 1973; Nishida & Fujii, 1976; Sanny et al., 1994). At the same time, the counterpart of the current sheet, that is, the growth phase arc, moves equatorward (Akasofu, 1964, 2010; Babu et al., 2024; Haerendel & Frey, 2021; Lessard et al., 2007). After the growth phase, the expansion phase is further characterized by the formation of positive or negative magnetic bays in ground-based

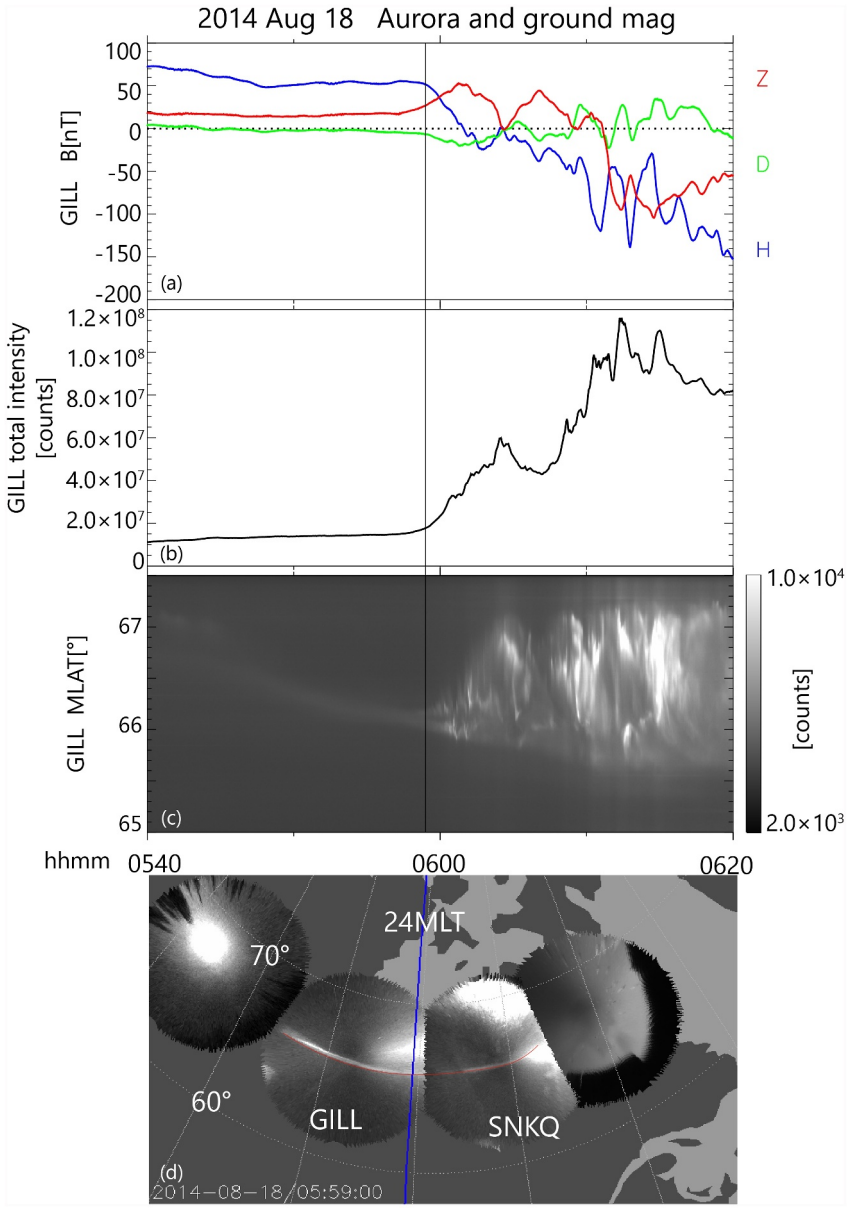


**Figure 1.** (a) Ground magnetometer data at GILL, (b) auroral intensity along the meridian of the GILL, (c) north–south keogram near the central meridian of the GILL THEMIS ASI, (d) THEMIS ASI snapshot at 05:59 UT during the substorm on 18 August 2014, the red curve corresponds to the auroral arc at 05:29 UT.

magnetometer data (Murphy et al., 2022); substorm aurora usually breaks up on the auroral arc that emerges in the growth phase in the premidnight sector, which sets the precondition for the substorm expansion phase (Liang et al., 2008; Lyons et al., 2002). This breakup is characterized by a sudden intensification of the arc followed by its fragmentation into multiple smaller structures. A prominent feature of the breakup is the westward surge—a rapid expansion of auroral emissions moving westward along the aurora oval during substorm events, where variations in auroral shape, intensity, and motion reflect changes in the magnetotail, such as energy accumulation during the growth phase and subsequent release during the expansion phase (Akasofu et al., 1965; Haerendel, 2015; Lyons et al., 2013; Ma et al., 2021), observing and characterizing these auroral features allows us to infer the timing, location, and mechanisms of magnetotail processes, offering a powerful diagnostic tool for understanding energy transport and conversion in the geospace environment.

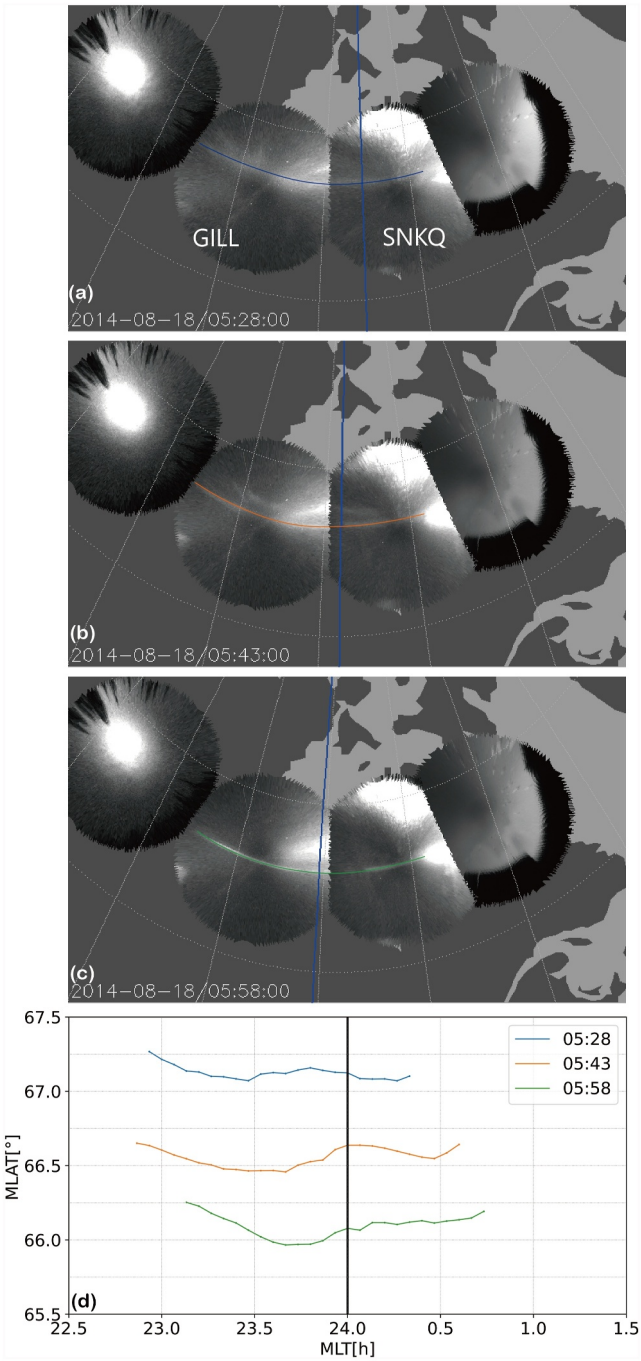


**Figure 2.** (a–c) The imager snapshot mosaics during the growth phase. The blue vertical lines are the magnetic midnight line, and the blue, orange, and green curves trace the arcs. (d) The blue curve corresponds to the auroral arc at 05:28 UT, the orange curve corresponds to the auroral arc at 05:43 UT and the green curve corresponds to the auroral arc at 05:58 UT.

In situ observations by spacecraft have shown that the magnetotail current sheet is thinner on the duskside (Artemyev et al., 2011; Zhang et al., 2024), which is caused by the Hall effect in the current sheet (Lu et al., 2016, 2018, 2019). The auroral substorm onset has also been observed to be located preferentially in the premidnight sector (Frey et al., 2004). Such duskside preference has also been shown in eastward-propagating auroral onset wave events and the quiet auroral arcs (Gillies et al., 2014; Nishimura et al., 2016). Therefore, it is important to examine the dawn-dusk morphology of the growth phase arcs so that one can bridge the magnetotail and auroral signatures of substorms from the growth phase to substorm onset. In this study, using the Time History of Events and Macroscale Interactions during Substorms (THEMIS) ASIs, we show that the growth phase arcs exhibit a morphological asymmetry in the dawn-dusk direction. They are at lower latitudes on the duskside, which is consistent with the thinner magnetotail current sheet on the duskside and the preferential substorm onset on the duskside.

## 2. Data and Methods

We use the THEMIS ASI data in 2014–2022 to observe the substorm growth phase arcs. The THEMIS ground-based ASI array observes the white light aurora over the North American continent from Canada to Alaska, the stations are located at geomagnetic latitudes between ∼60° and ∼70° [for example, Fort Simpson (FSIM, 67.30° magnetic latitude (MLAT) and 293.85° magnetic longitude (MLON)), Fort Smith (FSMI, 67.38° MLAT and 306.64° MLON), Gillam (GILL, 66.18° MLAT and 332.78° MLON) and Sanikiluaq (SNKQ, 66.45° MLAT and 356.99 MLON)]. The ASI array consists of 20 cameras covering a large section of the auroral oval with one-km resolution. The ASIs are time synchronized and have an image repetition rate of 3 s (Mende et al., 2008). Magnetometer data were obtained from both the THEMIS ground-based magnetometer array (Russell et al., 2008) and the Canadian Array for Realtime InvestigationS of Magnetic Activity (CARISMA) network (Mann et al., 2008). Stations used in this study include [for example, FSMI, GILL, and SNKQ] distributed across the auroral zone. The THEMIS ground magnetometers (GMAG) measure the magnetic field with 0.01 nT resolution at 2 samples/second, and we performed a 3-s smoothing of the geomagnetic field data in this study. The Geographic locations and more details of ASIs and GMAGs can be found on the official website (https://themis.igpp.ucla.edu). We use the ASI and magnetic field data provided by the instrument teams. We used software capable of measuring the smallest pixel point in the ASI image, the location of the edge of the auroral arc, identified by a sharp gradient in pixel brightness in the ASI image, and calculating a pair of geomagnetic latitude and geomagnetic longitude coordinates at 1 longitude interval.

The events of the substorm growth phase arcs are selected according to the following criteria: (a) clear, structurally stable auroral arcs distributed in both the dawn and dusk sectors throughout the whole growth phase; (b) the decrease in the ground magnetic field, the increase in the auroral intensity, and the intensification of the optical auroral forms should be synchronized. Following the above criteria, we screened the substorm events from 2014 to 2022 and obtained 47 substorm growth phase arcs (see Table S1 for event list). To better visualize the dawn-dusk morphology of the 47 arcs, precise latitude and longitude coordinates are extracted to analyze the exact location of the auroral arcs. We trace the trajectory of all the auroral arcs, taking a point at every longitude and recording the coordinates of these points.

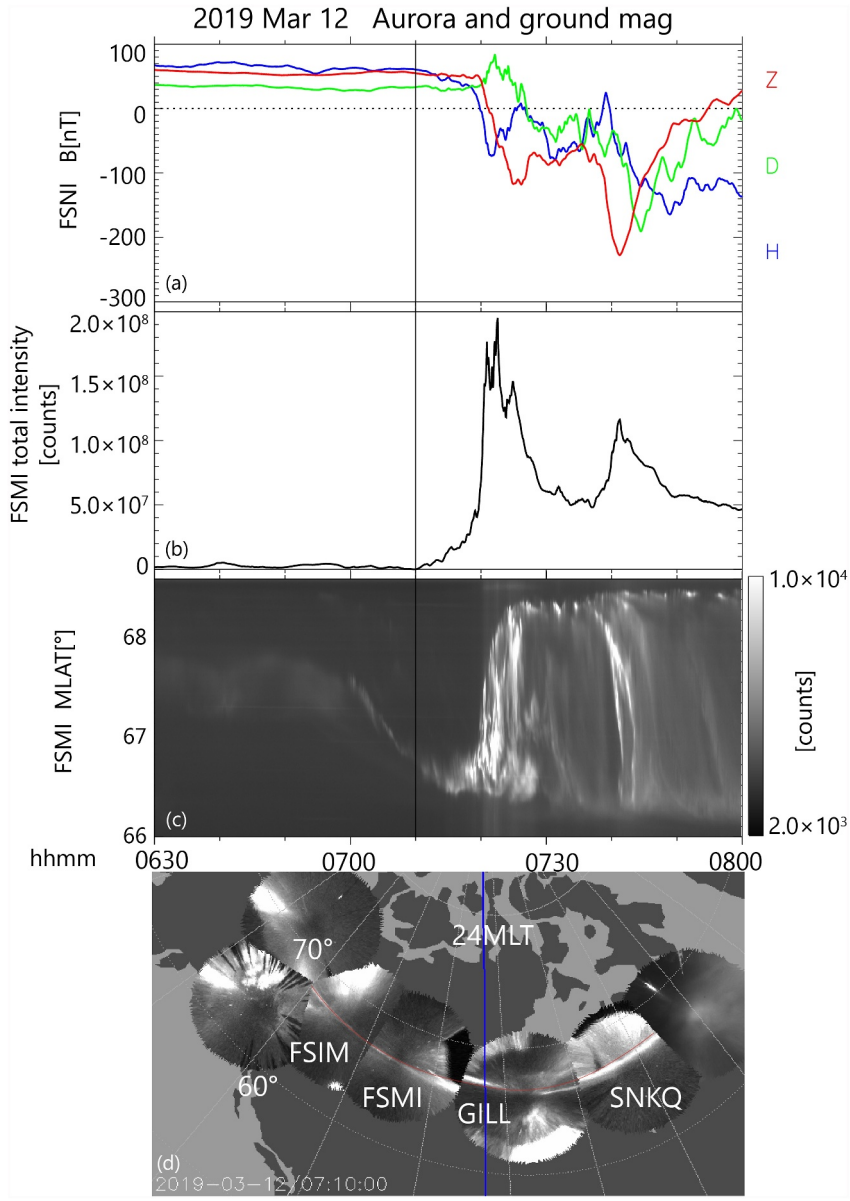


**Figure 3.** (a) Ground magnetometer data at FSMI, (b) auroral intensity along the meridian of the FSMI, (c) north-south keogram near the central meridian of the FSMI THEMIS ASI, (d) THEMIS ASI snapshot at 07:10 UT during the substorm on 12 March 2019, the red curve corresponds to the auroral arc at 07:10 UT.

## 3. Results

Figure 1 shows a representative substorm event, which was detected at GILL and SNKQ of the THEMIS array of ground-based observatories; the vertical line marks the initial rise of auroral intensity, that is, initial brightening (Nishimura et al., 2016, 2022), which coincides with intensification of optical auroral forms and decrease of the ground magnetic field (Figures 1a–1c). The geomagnetic field H component started to decrease around 05:59 UT and developed a negative bay. Until late in the expansion phase, H decreased by ∼220 nT, consistent with typical westward auroral electrojet signatures observed during substorm expansion phases (Gjerloev et al., 2003; Kamide & Kokubun, 1996; McPherron et al., 1973). Thus, it corresponds to the substorm growth phase before the initiation of the auroral brightening. The auroral arc moved equatorward before 05:59 UT, and then the arc started to brighten at ∼05:59 UT. The auroral arc is shown in the ASI snapshot at 05:59 UT, it was fully covered by the

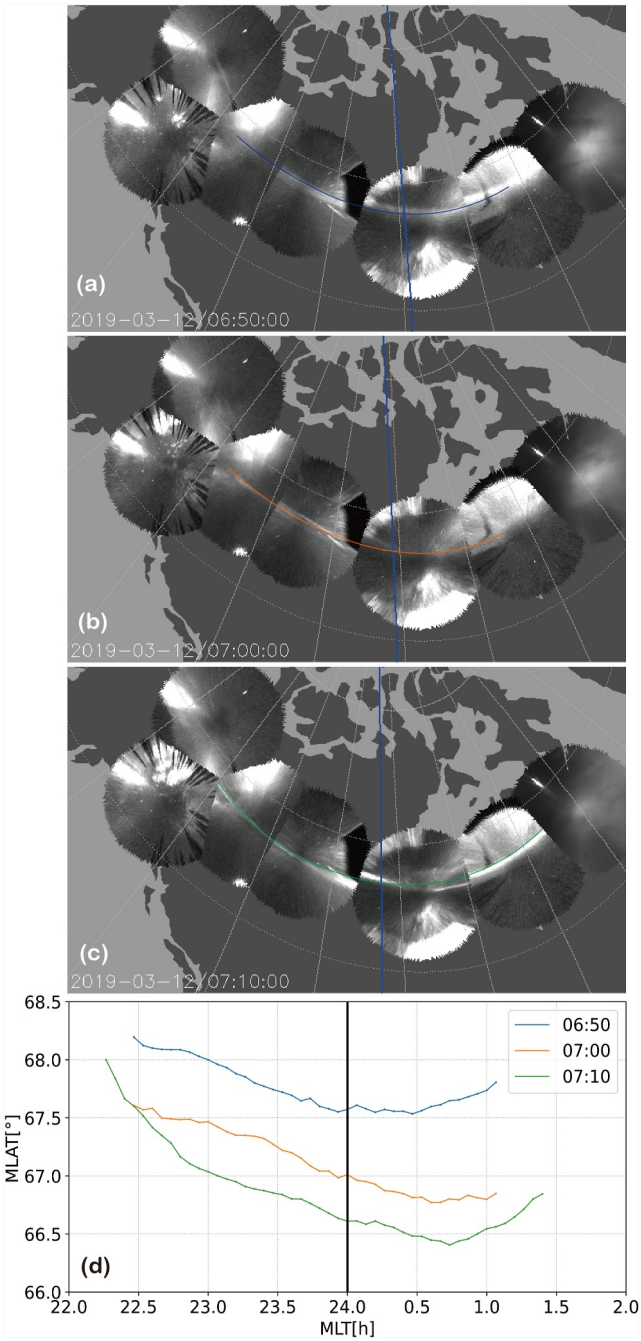


**Figure 4.** (a–c) The imager snapshot mosaics during the growth phase. The blue vertical lines are the magnetic midnight line, and the blue, orange, and green curves trace the arcs. (d) The blue curve corresponds to the auroral arc at 06:50 UT, 12 March 2019, the orange curve corresponds to the auroral arc at 07:00 UT; and the green curve corresponds to the auroral arc at 07:10 UT.

THEMIS ASI FOV near the GILL and SNKQ ASIs, and an east–west arc that spanned both the duskside and the dawnside can be seen clearly on the map (Figure 1d).

We chose three moments in the growth phase of this representative event (Figures 2a–2c), extracted the coordinates of the auroral arcs and plotted them in Figure 2d. Figure 2a corresponds to the early stage of the growth phase at 05:28 UT, when the structure of the auroral arc was just formed, at magnetic latitude of ~67.1°. At this time the auroral arc was at about the same latitude in the dawn and dusk sectors. At 05:43 UT (Figure 2b), that is, 15 min later, the auroral arc moved ~0.5° toward the equator, with slightly more equatorward displacement on the duskside. After another 15 min, at 05:58 UT (Figure 2c), which was within 1 min before the auroral expansion onset, the auroral arc already had a distinct latitudinal minimum and a greater curvature, and the latitudinal minimum of the arc was in the dusk sector, ~0.33 MLT from the meridian.

Similarly, another typical event occurred on 12 March 2019 shown in Figures 3 and 4. This auroral arc spanned a larger longitude and was observed in the field of view of four ASI stations: FSIM, FSMI, GILL and SNKQ. Starting at ~6:50 UT, the auroral arc continued to move equatorward for ~20 min before brightening. In this event, a latitudinal minimum occurred in the dawn sector. Of the 47 substorm events we selected, ~72.3% (34/47) had equatorward motion characteristics during the growth phase (the other 13 events are also included in the statistic). Some of the other 13 arcs exhibited clear poleward motion prior to onset, and some arcs didn't show apparent movement.

All the 47 growth phase arcs are presented in Figure 5a. The arcs are selected within the last 1 min of the growth phase. These arcs at the end of the growth phase are distributed over a latitude range from ~64.7° to ~68.7°, the red dots show the onset location of each auroral arc. It is evident that the location of the auroral onset is biased to the duskside, which is consistent with the results from the IMAGE mission (Frey et al., 2004). Figure 5b shows the occurrence frequency distribution of the MLT difference between each onset location and latitudinal minimum point (MLT difference = latitudinal minimum point MLT—onset location MLT). About 87% of events have an MLT difference value between −0.75 and 0.75 hr. The superposed growth phase arcs are shown in Figure 6, with the MLAT corresponding to 0 MLT being taken as the zero epoch MLAT (plots subtract the MLAT value at MLT = 0 of each line, while set ΔMLAT = 0 at MLT = 0). The red line is the average of all the arcs. The latitude of this averaged arc is a little lower in the dusk sector than in the dawn sector. Similar to the above representative case study, the statistical result also shows the dawn-dusk asymmetry of the growth phase arcs.

To quantitatively characterize the dawn-dusk asymmetry of the growth phase arcs, we show the MLT of latitudinal minimum points of all the 47 arcs in Figure 7a and the histogram in Figure 7b. The average of the latitudinal minimum points is at ~23.64 MLT, and the median is at 23.60 MLT. Most of the latitudinal minimum points of the growth phase arcs are located on the duskside (~74.5%), and only ~14.9% of them are on the dawnside. The rest ~10.6% are at magnetic midnight line. The duskmost point of the latitudinal minimum is at ~22.53 MLT, much farther than the dawn most point at ~0.87 MLT. The latitudinal minimum can be as low as ~65° on the duskside but is at higher latitude of above 66.5° on the dawnside.

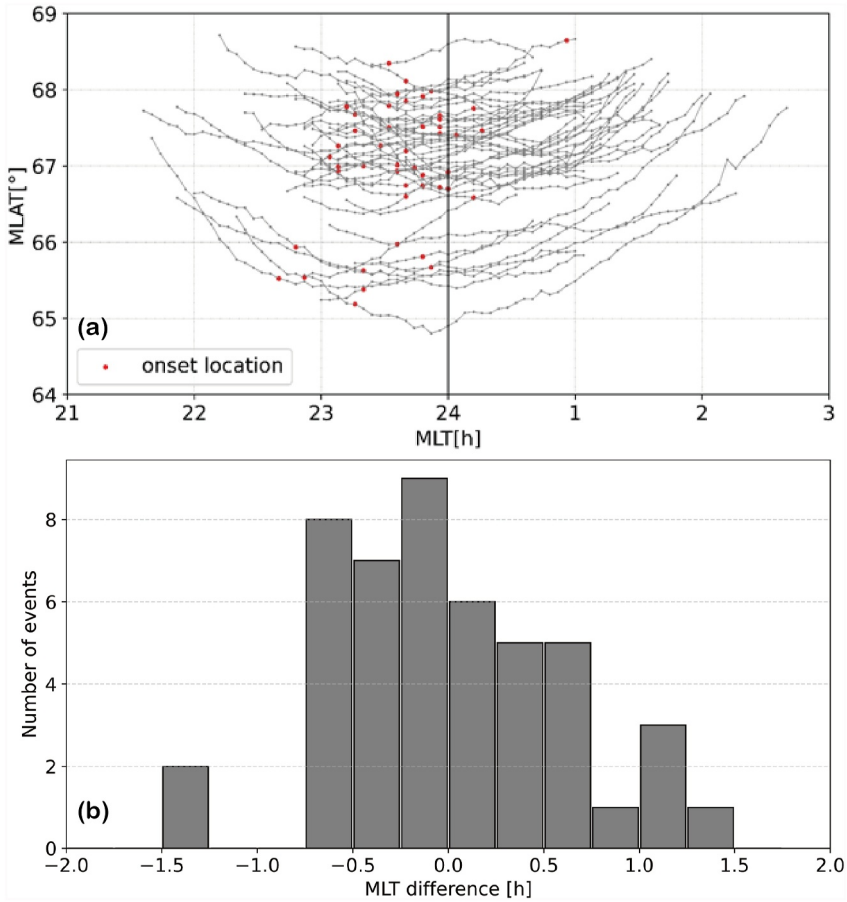


**Figure 5.** (a) Overview of the distribution of all the 47 growth phase arcs from 2014 to 2022. The black line is the magnetic midnight line, and red dots show the onset location of each event. (b) The occurrence frequency distribution of the MLT difference between each onset location and latitudinal minimum point. MLT difference = latitudinal minimum point MLT—onset location MLT.

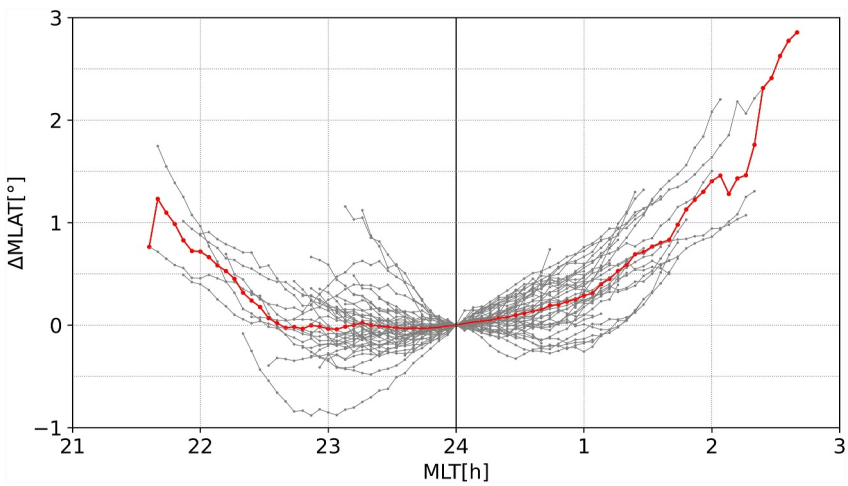


**Figure 6.** The result after superposing all the growth phase arcs, the red line is the average arc.

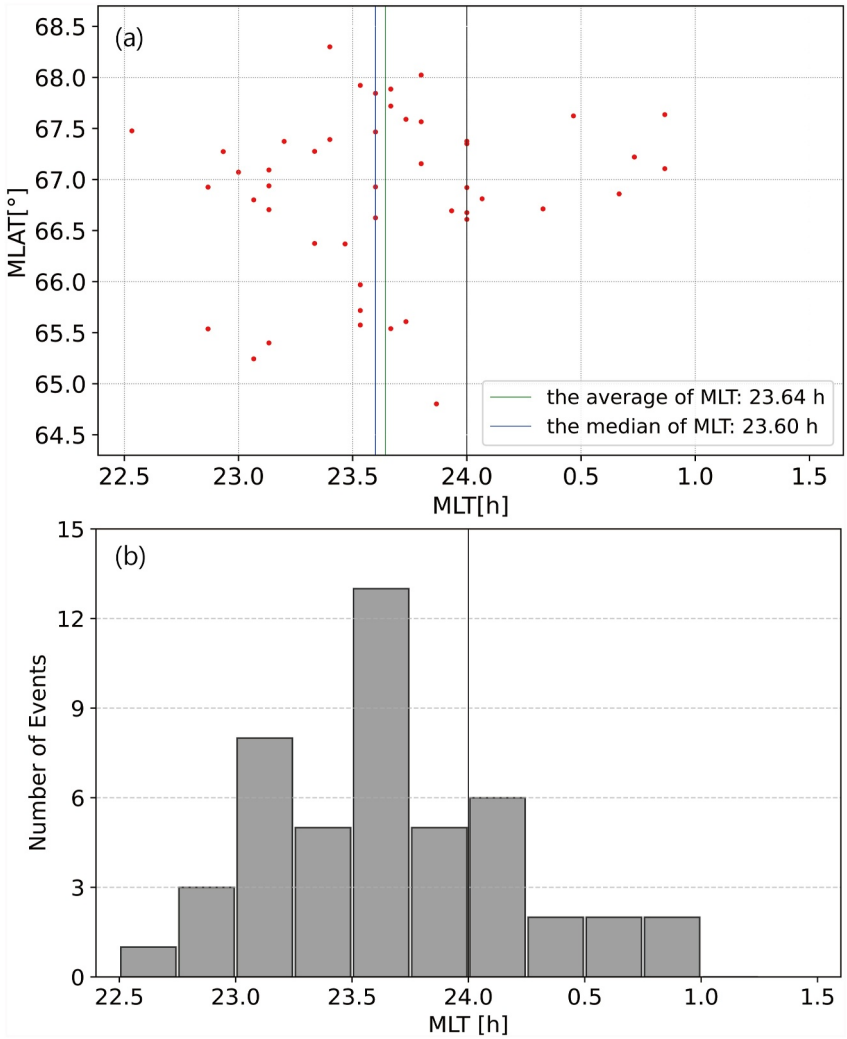


**Figure 7.** (a) Latitudinal minimum point of the arcs shown by red points. The vertical green line is the average MLT of the points, and the vertical blue line is the median MLT. (b) Histogram of the MLT of latitudinal minimum for all arcs.

## 4. Conclusions and Discussion

The morphological characteristics and evolutionary patterns of auroral arcs during the substorm growth phase are examined using THEMIS all-sky imager data of 47 substorm growth phase arcs from 2014 to 2022. Our findings reveal that the majority of auroral arcs (~72.3%) move equatorward during the growth phase, followed by an initial brightening in the midnight sector and then a substorm expansion onset. Based on a statistical study, the auroral arcs are found to develop a clear dawn-dusk asymmetry at the end of the growth phase. The arcs in the dusk sector are at lower latitudes, and most arcs have a latitudinal minimum preferentially on the duskside. This study reinforces the role of auroral morphology as an indicator of magnetospheric activity. By analyzing the evolution of auroral forms and their associated parameters, we gain valuable information about the state and dynamics of the magnetotail.

The dawn-dusk asymmetry is also observed in the magnetotail quiet current sheet, that is, the magnetotail is thinner on the duskside (Artemyev et al., 2011; Rong et al., 2011; Vasko et al., 2015; Zhang et al., 2024), and the thinner current sheet may extend closer to the Earth on the dusk side as shown in the simulations by Lu et al. (2016). More specifically, a recent statistical study by Zhang et al. (2024) showed that the magnetotail current sheet is the thinnest on the duskside, at $x$~–22 $R_E$, $y$~7 $R_E$ in the GSM (Geocentric Solar-Magnetospheric) coordinate system. This location corresponds to ~23 MLT. In the study presented here, the minimum latitude of the average preonset arc established in Figure 6 also in the premidnight sector at around 23 MLT. This indicates a

distinct asymmetry which collaborates that found by Sergeev et al. (2020). Such dawn-dusk asymmetries are also consistent with that of the substorm onset with a peak occurrence rate at ∼23 MLT (Frey et al., 2004, and Figure 5a in the present study as well), showing that substorm onset occurs preferentially when the growth phase arc is at lower latitude and the current sheet is thinner. This is also correlated to the higher occurrence rate of magnetotail reconnection and transients on the duskside (e.g., Eastwood et al., 2010; Imber et al., 2011; Liu et al., 2013). Moreover, there are also some geomagnetic asymmetric features associated with substorms. The MLT differences observed in the statistical results may be attributed to the magnetosphere–ionosphere (M–I) coupling process. The auroral initial brightening is not solely a consequence of local plasma dynamics; rather, it results from a globally coupled system in which the field-aligned currents (FACs) are governed by shear flows between the magnetosphere and the ionosphere (Ebihara & Tanaka, 2015; Tanaka, 2015). The ground signatures of the magnetospheric convection have specific asymmetry in MLT; the temporal variations of the ground magnetic field (dB/dt) show an occurrence maximum in premidnight (22–23 MLT), which is related to the substorm expansion phase (Apatenkov et al., 2004). Similar MLT distributions are observed for the geomagnetically induced currents (GIC) caused by rapid magnetic field variations (Viljanen et al., 2014). Another structure with a clear dawn-dusk asymmetry is electron isotropy boundaries (IBs) associated electron precipitation from the inner edge of the thin current sheets (see details in Sergeev et al., 2012; and references therein). The latitudinally averaged precipitation energy flux associated with IBs and the contribution to total high-latitude precipitation power peaks around 22 MLT (Wilkins et al., 2023), the peak electron IB emergence on the MLT and the precipitation energy peak statistically collocated with the substorm onset MLT. The dawn-dusk asymmetries of the above phenomena constitute the systematic duskside preference of the magnetospheric dynamics, which are also monitored on the ionosphere by the auroral activities.

## Data Availability Statement

THEMIS data used in this study can be obtained from http://themis.ssl.berkeley.edu as daily CDF files. Data access and processing were performed using SPEDAS V4.1 (Angelopoulos et al., 2019).

**Acknowledgments**
This research was funded by the NSFC Grants 42274196, 42230201, and the Strategic Priority Research Program of the Chinese Academy of Sciences (Grants XDB0560000 and XDB41000000). We thank ISSI through the International Team project, Magnetotail Dipolarizations: Archimedes Force or Ideal Collapse.

## References

Akasofu, S.-I. (1964). The development of the auroral substorm. *Planetary and Space Science*, *12*(4), 273–282. https://doi.org/10.1016/0032-0633(64)90151-5

Akasofu, S.-I., Kimball, D. S., & Meng, C.-I. (1965). The dynamics of the aurora—II. Westward traveling surges. *Journal of Atmospheric and Terrestrial Physics*, *27*(2), 173–180. https://doi.org/10.1016/0021-9169(65)90114-5

Akasofu, S.-I., Lui, A. T. Y., & Meng, C.-I. (2010). Importance of auroral features in the search for substorm onset processes. *Journal of Geophysical Research*, *115*(A8), A08218. https://doi.org/10.1029/2009JA014960

Angelopoulos, V., Cruce, P., Drozdov, A., Grimes, E. W., Hatzigeorgiu, N., King, D. A., et al. (2019). The Space Physics Environment Data Analysis System (SPEDAS) (version 4.1) [Software]. *Space Science Reviews*, *215*(1), 9. https://doi.org/10.1007/s11214-018-0576-4

Apatenkov, S. V., Sergeev, V. A., Pirjola, R., & Viljanen, A. (2004). Evaluation of the geometry of ionospheric current systems related to rapid geomagnetic variations. *Annals of Geophysics*, *22*(1), 63–72. https://doi.org/10.5194/angeo-22-63-2004

Artemyev, A. V., Petrukovich, A. A., Nakamura, R., & Zelenyi, L. M. (2011). Cluster statistics of thin current sheets in the Earth Magnetotail: Specifics of the dawn flank, proton temperature profiles and electrostatic effects. *Journal of Geophysical Research*, *116*(A9), A09233. https://doi.org/10.1029/2011JA016801

Babu, S. S., Mann, I. R., Donovan, E. F., Smith, A. W., Dimitrakoudis, S., Sydora, R. D., & Kale, A. (2024). Plasma sheet counterparts for auroral beads and vortices in advance of fast flows: New evidence for near-Earth substorm onset. *Journal of Geophysical Research: Space Physics*, *129*(6), e2023JA031957. https://doi.org/10.1029/2023JA031957[

Baker, D. N., Pulkkinen, T. I., Angelopoulos, V., Baumjohann, W., & McPherron, R. L. (1996). Neutral line model of substorms: Past results and present view. *Journal of Geophysical Research*, *101*(A6), 12975–13010. https://doi.org/10.1029/95JA03753

Borovsky, J. E. (1993). Auroral arc thicknesses as predicted by various theories. *Journal of Geophysical Research*, *98*(A4), 6101–6138. https://doi.org/10.1029/92ja02242

Caan, M. N., McPherron, R. L., & Russell, C. (1975). Substorm and interplanetary magnetic field effects on the geomagnetic tail lobes. *Journal of Geophysical Research*, *80*(1), 191–194. https://doi.org/10.1029/JA080i001p00191

Caan, M. N., McPherron, R. L., & Russell, C. T. (1973). Solar wind and substorm-related changes in the lobes of the geomagnetic tail. *Journal of Geophysical Research*, *78*(34), 8087–8096. https://doi.org/10.1029/JA078i034p08087

Caan, M. N., McPherron, R. L., & Russell, C. T. (1977). Characteristics of the association between interplanetary magnetic field and substorms. *Journal of Geophysical Research*, *82*(29), 4837–4842. https://doi.org/10.1029/JA082i029p04837

Chen, L., Shiokawa, K., Miyoshi, Y., Oyama, S., Jun, C.-W., Ogawa, Y., et al. (2022). Observation of source plasma and field variations of a substorm brightening aurora at L ∼ 6 by a ground-based camera and the arase satellite on 12 October 2017. *Journal of Geophysical Research: Space Physics*, *127*(11), e2021JA030072. https://doi.org/10.1029/2021JA030072

Cowley, S., & Lockwood, M. (1992). Excitation and decay of solar wind-driven flows in the magnetosphere-ionosphere system. *Annales Geophysicae*, *10*, 103–115.

Eastwood, J. P., Phan, T. D., Oieroset, M., & Shay, M. A. (2010). Average properties of the magnetic reconnection ion diffusion region in the Earth's Magnetotail: The 2001–2005 cluster observations and comparison with simulations. *Journal of Geophysical Research*, *115*(A8), A08215. https://doi.org/10.1029/2009JA014962

Ebihara, Y., & Tanaka, T. (2015). Substorm simulation: Insight into the mechanisms of initial brightening. *Journal of Geophysical Research: Space Physics*, *120*(9), 7270–7288. https://doi.org/10.1002/2015JA021516

Fairfield, D. H., Hones, E. W., Jr., & Meng, C.-I. (1981). Multiple crossings of a very thin plasma sheet in the Earth's magnetotail. *Journal of Geophysical Research*, *86*(A13), 11189–11200. https://doi.org/10.1029/JA086iA13p11189

Foster, J., Fairfield, D., Ogilvie, K., & Rosenberg, T. (1971). Relationship of interplanetary parameters and occurrence of magnetospheric substorms. *Journal of Geophysical Research*, *76*(28), 6971–6975. https://doi.org/10.1029/JA076i028p06971

Frey, H. U., Mende, S. B., Angelopoulos, V., & Donovan, E. F. (2004). Substorm onset observations by IMAGE-FUV. *Journal of Geophysical Research*, *109*(A10), A10304. https://doi.org/10.1029/2004JA010607

Gillies, D. M., Knudsen, D. J., Donovan, E. F., Spanswick, E. L., Hansen, C., Keating, D., & Erion, S. (2014). A survey of quiet auroral arc orientation and the effects of the interplanetary magnetic field. *Journal of Geophysical Research: Space Physics*, *119*(4), 2550–2562. https://doi.org/10.1002/2013JA019469

Gjerloev, J. W., Hoffman, R. A., Tanskanen, E., Friel, M., Frank, L. A., & Sigwarth, J. B. (2003). Auroral electrojet configuration during substorm growth phase. *Geophysical Research Letters*, *30*(18), 1927. https://doi.org/10.1029/2003GL017851

Haerendel, G. (2015). Flow bursts, breakup arc, and substorm current wedge. *Journal of Geophysical Research: Space Physics*, *120*(4), 2796–2807. https://doi.org/10.1002/2014JA020954

Haerendel, G., & Frey, H. (2021). The onset of a substorm and the mating instability. *Journal of Geophysical Research: Space Physics*, *126*(10), e2021JA029492. https://doi.org/10.1029/2021JA029492

Imber, S. M., Slavin, J. A., Auster, H. U., & Angelopoulos, V. (2011). A THEMIS survey of flux ropes and traveling compression regions: Location of the near-Earth reconnection site during solar minimum. *Journal of Geophysical Research*, *116*(A2), A02201. https://doi.org/10.1029/2010JA016026

Kallio, E. I., Pulkkinen, T. I., Koskinen, H. E. J., Viljanen, A., Slavin, J. A., & Ogilvie, K. (2000). Loading-unloading processes in the nightside ionosphere. *Geophysical Research Letters*, *27*(11), 1627–1630. https://doi.org/10.1029/1999GL003694

Kamide, Y., & Kokubun, S. (1996). Two-component auroral electrojet: Importance for substorm studies. *Journal of Geophysical Research*, *101*(A6), 13027–13046. https://doi.org/10.1029/96JA00142

Kauristie, K., Syrjäsuo, M., Amm, O., Viljanen, A., Pulkkinen, T., & Opgenoorth, H. (2001). A statistical study of evening sector arcs and electrojets. *Advances in Space Research*, *28*(11), 1605–1610. https://doi.org/10.1016/S0273-1177(01)00480-X

Knudsen, D., Donovan, E., Cogger, L., Jackel, B., & Shaw, W. (2001). Width and structure of mesoscale optical auroral arcs. *Geophysical Research Letters*, *28*(4), 705–708. https://doi.org/10.1029/2000gl011969

Lessard, M. R., Lotko, W., LaBelle, J., Peria, W., Carlson, C. W., Creutzberg, F., & Wallis, D. D. (2007). Ground and satellite observations of the evolution of growth phase auroral arcs. *Journal of Geophysical Research*, *112*(A9), A09304. https://doi.org/10.1029/2006JA011794

Liang, J., Donovan, E. F., Liu, W. W., Jackel, B., Syrjäsuo, M., Mende, S. B., et al. (2008). Intensification of preexisting auroral arc at substorm expansion phase onset: Wave-like disruption during the first tens of seconds. *Geophysical Research Letters*, *35*(17), L17S19. https://doi.org/10.1029/2008GL033666

Liu, J., Angelopoulos, V., Runov, A., & Zhou, X. Z. (2013). On the current sheets surrounding dipolarizing flux bundles in the magnetotail: The case for wedgelets. *Journal of Geophysical Research: Space Physics*, *118*(5), 2000–2020. https://doi.org/10.1002/jgra.50092

Lu, S., Pritchett, P. L., Angelopoulos, V., & Artemyev, A. V. (2018). Formation of dawn-dusk asymmetry in Earth's magnetotail thin current sheet: A three-dimensional particle-in-cell simulation. *Journal of Geophysical Research: Space Physics*, *123*(4), 2801–2814. https://doi.org/10.1002/2017ja025095

Lu, S., Artemyev, A. V., Angelopoulos, V., Lin, Y., Zhang, X.-J., Liu, J., et al. (2019). The Hall electric field in Earth's magnetotail thin current sheet. *Journal of Geophysical Research: Space Physics*, *124*(2), 1052–1062. https://doi.org/10.1029/2018JA026202

Lu, S., Lin, Y., Angelopoulos, V., Artemyev, A. V., Pritchett, P. L., Lu, Q., & Wang, X. Y. (2016). Hall Effect control of magnetotail dawn-dusk asymmetry: A three-dimensional global hybrid simulation. *Journal of Geophysical Research: Space Physics*, *121*(12), 11882–11895. https://doi.org/10.1002/2016JA023325

Lyons, L. R., Nishimura, Y., Gallardo-Lacourt, B., Zou, Y., Donovan, E., Mende, S., et al. (2013). Westward traveling surges: Sliding along boundary arcs and distinction from onset arc brightening. *Journal of Geophysical Research: Space Physics*, *118*(12), 7643–7653. https://doi.org/10.1002/2013JA019334

Lyons, L. R., Voronkov, I. O., Donovan, E. F., & Zesta, E. (2002). Relation of substorm breakup arc to other growth-phase auroral arcs. *Journal of Geophysical Research*, *107*(A11), SMP26-1–SMP26-10. https://doi.org/10.1029/2002JA009317

Ma, Y., Zhang, Q., Lyons, L. R., Liu, J., Xing, Z., Reimer, A., et al. (2021). Is westward travelling surge driven by the polar cap flow channels? *Journal of Geophysical Research: Space Physics*, *126*(8), e2020JA028498. https://doi.org/10.1029/2020JA028498

Mann, I. R., Milling, D. K., Rae, I. J., Ozeke, L. G., Kale, A., Kale, Z. C., et al. (2008). The upgraded CARISMA magnetometer array in the THEMIS era. *Space Science Reviews*, *141*(1–4), 413–451. https://doi.org/10.1007/s11214-008-9457-6

McPherron, R. L. (1970). Growth phase of magnetospheric substorms. *Journal of Geophysical Research*, *75*(28), 5592–5599. https://doi.org/10.1029/JA075i028p05592

McPherron, R. L. (1979). Magnetospheric substorms. *Reviews of Geophysics*, *17*(4), 657–681. https://doi.org/10.1029/RG017i004p00657

McPherron, R. L., Russell, C. T., & Aubry, M. P. (1973). Satellite studies of magnetospheric substorms on August 15, 1968: 9. Phenomenological model for substorms. *Journal of Geophysical Research*, *78*(16), 3131–3149. https://doi.org/10.1029/JA078i016p03131

Mende, S. B., Harris, S. E., Frey, H. U., Angelopoulos, V., Russell, C. T., Donovan, E., et al. (2008). The THEMIS array of ground-based observatories for the study of auroral substorms. *Space Science Reviews*, *141*(1–4), 357–387. https://doi.org/10.1007/s11214-008-9380-x

Motoba, T., Ohtani, S., Anderson, B. J., Korth, H., Mitchell, D., Lanzerotti, L. J., et al. (2015). On the formation and origin of substorm growth phase/onset auroral arcs inferred from conjugate space-ground observations. *Journal of Geophysical Research: Space Physics*, *120*(10), 8707–8722. https://doi.org/10.1002/2015JA021676

Murphy, K. R., Bentley, S. N., Miles, D. M., Sandhu, J. K., & Smith, A. W. (2022). Imaging the magnetosphere–ionosphere system with ground-based and in situ magnetometers. In *Magnetospheric imaging* (pp. 287–340). Elsevier. https://doi.org/10.1016/B978-0-12-820630-0.00002-7

Nishida, A., & Fujii, K. (1976). Thinning of the near-earth (10 ∼15 RE) plasma sheet preceding the substorm expansion phase. *Planetary and Space Science*, *24*(9), 849–853. https://doi.org/10.1016/0032-0633(76)90075-1

Nishimura, Y., Artemyev, A. V., Lyons, L. R., Gabrielse, C., Donovan, E. F., & Angelopoulos, V. (2022). Space-ground observations of dynamics of substorm onset beads. *Journal of Geophysical Research: Space Physics*, *127*(2), e2021JA030004. https://doi.org/10.1029/2021JA030004

Nishimura, Y., Lyons, L. R., Kikuchi, T., Angelopoulos, V., Donovan, E., Mende, S., et al. (2012). Formation of substorm Pi2: A coherent response to auroral streamers and currents. *Journal of Geophysical Research*, *117*(A9), A09218. https://doi.org/10.1029/2012JA017889

Nishimura, Y., Lyons, L. R., Zou, S., Xing, X., Angelopoulos, V., Mende, S. B., et al. (2010). Preonset time sequence of auroral substorms: Coordinated observations by all-sky imagers, satellites, and radars. *Journal of Geophysical Research*, *115*(A5), A00I08. https://doi.org/10.1029/2010JA015832

Nishimura, Y., Yang, J., Pritchett, P. L., Coroniti, F. V., Donovan, E. F., Lyons, L. R., et al. (2016). Statistical properties of substorm auroral onset beads/rays. *Journal of Geophysical Research: Space Physics*, *121*(9), 8661–8676. https://doi.org/10.1002/2016JA022801

Pulkkinen, T. I., Koskinen, H. E. J., & Pellinen, R. J. (1991). Mapping of auroral arcs during substorm growth phase. *Journal of Geophysical Research*, *96*(A12), 21087–21094. https://doi.org/10.1029/91JA01960

Rong, Z. J., Wan, W. X., Shen, C., Li, X., Dunlop, M. W., Petrukovich, A. A., et al. (2011). Statistical survey on the magnetic structure in magnetotail current sheets. *Journal of Geophysical Research*, *116*(A9), A09218. https://doi.org/10.1029/2011JA016489

Russell, C. T., Chi, P. J., Dearborn, D. J., Ge, Y. S., Kuo-Tiong, B., Means, J. D., et al. (2008). THEMIS ground-based magnetometers. *Space Science Reviews*, *141*(1–4), 389–412. https://doi.org/10.1007/s11214-008-9337-0

Sanny, J., McPherron, R. L., Russell, C. T., Baker, D. N., Pulkkinen, T. I., & Nishida, A. (1994). Growth-phase thinning of the near-Earth current sheet during the CDAW 6 substorm. *Journal of Geophysical Research*, *99*(A4), 5805–5816. https://doi.org/10.1029/93JA03235

Sergeev, V., Bondareva, T., Gilles, D., & Donovan, E. (2020). On the source region and orientation of the nightside auroral arcs. *Journal of Atmospheric and Solar-Terrestrial Physics*, *204*, 105288. https://doi.org/10.1016/j.jastp.2020.105288

Sergeev, V., Nishimura, Y., Kubyshkina, M., Angelopoulos, V., Nakamura, R., & Singer, H. (2012). Magnetospheric location of the equatorward prebreakup arc. *Journal of Geophysical Research*, *117*(A1), A01212. https://doi.org/10.1029/2011JA017154

Tanaka, T. (2015). Substorm auroral dynamics reproduced by advanced global magnetosphere−ionosphere (M–I) coupling simulation. In Y. Zhang & L. J. Paxton (Eds.), *Geophysical monograph series* (1st ed., pp. 177–190). https://doi.org/10.1002/9781118978719.ch13

Vasko, I. Y., Petrukovich, A. A., Artemyev, A. V., Nakamura, R., & Zelenyi, L. M. (2015). Earth's distant magnetotail current sheet near and beyond lunar orbit. *Journal of Geophysical Research: Space Physics*, *120*(10), 8663–8680. https://doi.org/10.1002/2015JA021633

Viljanen, A., Pirjola, R., Prácser, E., Katkalov, J., & Wik, M. (2014). Geomagnetically induced currents in Europe-modelled occurrence in a continent-wide power grid. *Journal of Space Weather and Space Climate*, *4*, A09. https://doi.org/10.1051/swsc/2014006

Wilkins, C., Angelopoulos, V., Runov, A., Artemyev, A., Zhang, X.-J., Liu, J., & Tsai, E. (2023). Statistical characteristics of the electron isotropy boundary. *Journal of Geophysical Research: Space Physics*, *128*(10), e2023JA031774. https://doi.org/10.1029/2023JA031774

Zhang, Z., Lu, S., Lu, Q., Wang, R., Zhan, C., Li, X., & Artemyev, A. V. (2024). Statistical survey of thin current sheets in Earth's magnetotail: MMS observations. *Journal of Geophysical Research: Space Physics*, *129*(5), e2024JA032575. https://doi.org/10.1029/2024JA032575